Proc. Natl. Acad. Sci. USA
Vol. 82, pp. 3504–3508, May 1985
Neurobiology

Evidence that receptors mediating central synaptic potentials extend beyond the postsynaptic density

(synaptic receptors/quantal responses)

DONALD S. FABER*, PAUL G. FUNCH*, AND HENRI KORN†

*Division of Neurobiology, Department of Physiology, State University of New York, 313 Cary Hall, Buffalo, NY 14214; and †Institut National de la Santé et de la Recherche Médicale U261, Department de Biologie Moleculaire, Institut Pasteur, 25 Rue du Docteur Roux, 75724 Paris Cedex 15, France

Communicated by E. E. Salpeter, January 14, 1985

ABSTRACT **Physiological recordings and computer simulations of unitary inhibitory postsynaptic potentials in the Mauthner cell of the goldfish central nervous system have been used to estimate the expected size of the postsynaptic receptor matrix at individual junctions. Simultaneous pre- and postsynaptic recordings were used to determine the kinetic parameters of the quantal responses under normal conditions and in the presence of strychnine, a competitive antagonist of glycine, which is the putative transmitter at these synapses. Calculations indicate that if the postsynaptic density, which has a radius of 0.1 μm, were to accommodate the population of channels estimated to be opened during a quantal response, the glycine binding site density in that region would be unrealistically high. Computer simulation of the quantal responses included transmitter diffusion, transmitter–receptor interactions, and channel activation under conditions including both normal and lowered binding site densities, the latter corresponding to the experimental data obtained with strychnine. The data indicate that the synaptic receptors involved in generating unitary responses are widely distributed to include regions located outside the junctional area, which directly faces the presynaptic release sites. We further suggest that the receptor matrix is surrounded by a restricted diffusional space; this geometrical organization may underlie the finding that response rise times are relatively independent of receptor binding site densities.**

Physiological comparisons between the postsynaptic organization of central and peripheral junctions have been hampered by a lack of direct experimental access to synapses of the central nervous system (CNS). On the basis of ultrastructural observations, it is generally assumed (1–3) that in the CNS the synaptic receptors involved in the generation of postsynaptic responses are restricted to the area delimited by the postsynaptic density (psd), which is in direct apposition to, and essentially coextensive with, the presynaptic active zone or release site. This assertion has provided one rationale for postulating that the effects of adjacent synapses are independent of each other. However, we present evidence suggesting that the matrix containing a high density of receptors actually extends far beyond the limits of the psd, so as to include the so-called peri-synaptic region (3). Indeed, it appears that the receptors in both zones are necessarily involved in the normal generation of synaptic responses and must be considered as intrinsic to the central synaptic unit. The suggestion that this unit requires a wider spatial definition may redirect searches for (*i*) an adequate morphological marker of the receptor matrix, and (*ii*) postjunctional factors influencing synaptic efficacy, particularly in certain instances of plasticity (4–6).

The publication costs of this article were defrayed in part by page charge payment. This article must therefore be hereby marked "*advertisement*" in accordance with 18 U.S.C. §1734 solely to indicate this fact.

MATERIALS AND METHODS

Electrophysiological Preparation. Data were obtained in a physiologically and structurally well-defined system—namely, inhibitory synapses onto the goldfish (*Carassius auratus*) Mauthner cell (M cell). This preparation has been used to make simultaneous intracellular recordings from identified pre- and postsynaptic neurons (7) and histological reconstructions of the dye-injected presynaptic cells (8, 9). Recordings from the M-cell soma were made with KCl-filled microelectrodes in order to increase intracellular Cl^- ion concentration; consequently, the Cl^--dependent inhibitory postsynaptic potentials (IPSPs), which are otherwise undetectable (7), were depolarizing. The time course and quantal properties of the small unitary responses (several mV at most) are well known from previous studies (8–11). Similarly, the synapses involved in the generation of these potentials have been characterized at the light and electron microscopic levels: a presynaptic cell issues from 3 to ≈100 terminals (radius, 0.5–2.5 μm), each containing a single presynaptic grid or active zone apposing a comparably sized (radius, ≈0.1 μm) psd (12).

Computer Simulation. Our program for simulating CNS unitary potentials is based on that developed for analyzing miniature endplate currents at the amphibian neuromuscular junction (13, 14), which models radial transmitter diffusion over a large synaptic disk (15) containing a uniform density, σ, of receptors, assuming two binding sites per channel. Two general modifications were thus required for that program to be applicable to central synapses: (*i*) the width of the synaptic cleft was taken as 20 nm (ref. 12; ref. 16, p. 124 and pp. 135–136), and (*ii*) diffusion was considered to be along the whole synaptic contact zone, which could include a receptor-free annulus surrounding the "active" central disk. Receptor binding was modeled as a two-step reaction, with forward and backward rate constants of k_{+1}, k_{+2} and k_{-1}, k_{-2}, respectively. Many sets of model parameters were evaluated for their ability to reproduce the kinetics and magnitude of unitary IPSPs, as discussed below. The major common constraints were (*i*) that the rate constants be consistent with published estimates of the affinity of the glycine receptor for glycine (20–40 μM; see ref. 17), (*ii*) that parameter k_{-2} take into consideration the idea that response decay time is determined by mean channel lifetime (10, 11, 18), and (*iii*) that the diffusion coefficient be less than or equal to that for free diffusion of a small ion in water. It should be noted that the parameter k_{+2} incorporates a second binding step and channel opening, with the former assumed to be rate limiting. Simulated responses were then generated for conditions in which the amount of transmitter contained in a single synaptic vesicle varied from 5000 to 20,000 molecules, which is in the range of values reported for the neuromuscular

Abbreviations: CNS, central nervous system; M cell, Mauthner cell; IPSP, inhibitory postsynaptic potential; psd, postsynaptic density.

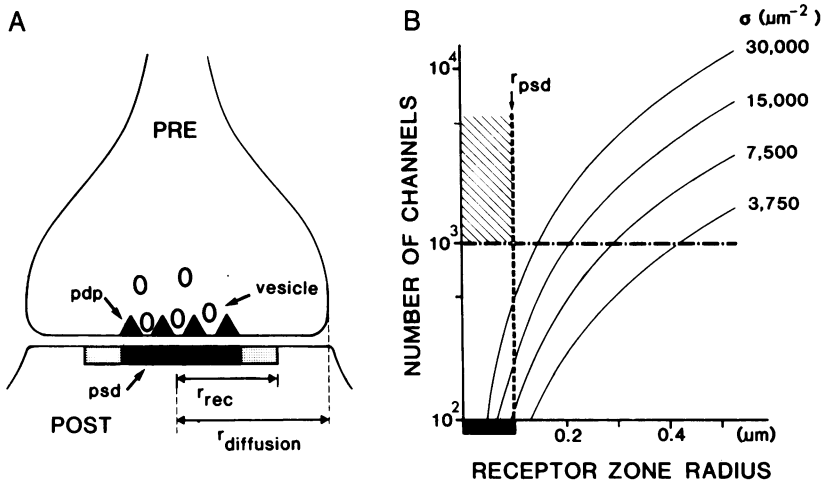

FIG. 1. A structural model for CNS synapses and comparison of the dimensions of postsynaptic specializations with those required for the receptor matrix. (*A*) Scheme of a synapse established between a presynaptic bouton (PRE) and its target cell (POST). Transmitter, packaged in vesicles, is released by exocytosis at the active zone, which is identified by presynaptic dense projections (pdp) and is in apposition to the psd (solid bar). The model used to simulate synaptic responses considers that the radius (r_{rec}) of the postsynaptic receptor matrix may be greater than that of the psd. It also incorporates transmitter diffusion along a receptor-free annulus, the width of which equals ($r_{diffusion} - r_{rec}$), with the former being defined by the total contact zone between pre- and postsynaptic elements. (*B*) Steady-state plots of the number of channels in the receptor zone, as a function of its radius and of binding site density, σ. Calculations were based on evidence for one channel per two receptor binding sites (20, 21). Vertical and horizontal dashed lines designate the radius of the psd (r_{psd}; thick bar) in the M cell and the criterion of involvement of at least 1000 channels in its quantal inhibitory responses, respectively. In no case does a region as large as the psd (hatched region) accommodate a sufficient number of channels. For example, even with an assumed binding site density of as much as 15,000 μm^{-2}, the requisite radius is twice that of the psd.

junction (19) and is assumed to pertain to these central glycinergic synapses as well. Finally, the model did not incorporate a mechanism for inactivating the transmitter, as there is no compelling evidence for such an action at these junctions.

RESULTS

The arguments that make it likely that the receptor matrix extends beyond the region delineated by the psd derive, in part, from the quantal properties of the release mechanism, as revealed with a binomial analysis of fluctuating unitary IPSPs. As estimated previously, the peak conductance change during the quantal response due to release of the putative transmitter glycine (20, 21) at a single terminal such as that illustrated in Fig. 1*A*, involves the opening of about 1500 Cl^- channels, and this effect was attributed to the transmitter content of one synaptic vesicle (8, 9). This estimate was obtained with two independent calculations, both of which were based on the evidence that the amplitude of the full-sized IPSP produced by activation of the M cell's collateral network typically is one-half of the driving force and that this neuron's input conductance is 6.08×10^{-6} S (11). First, the mean value of the quantum size, which is 1.15% of the collateral IPSP, could be converted to a peak conductance of 3.5×10^{-8} S. Second, the average unitary IPSP, which is 5.5% of the collateral response and has a mean quantal content of 3.25, corresponds to a peak quantal conductance of 5.2×10^{-8} S. Assuming a single glycine-activated Cl^- channel conductance of 25 pS (see discussion in ref. 11), we calculated that the average number of channels opened by one releasing bouton was 1400 and 2100, respectively (9). A third calculation, based on the maximal shunting of the passively conducted antidromic action potential in the M-cell soma (11), gave a unitary conductance between those two calculated above. Recent findings that such channels may have multiple conductances ranging from 20 to 45 pS (22, 23) could at most lower these estimates to as few as 1000 channels. Hence, simple calculations were used to determine the extent of the postsynaptic membrane required to accommodate these 1000 channels.

Assuming that the receptor matrix can be treated as a disk, of radius r_{rec}, the total number of channels, N, contained in that area equals $\sigma\pi(r_{rec})^2/n$, where n = the number of binding sites per receptor–channel complex. The latter parameter has been estimated with iontophoresis of glycine (20, 21) and from single channel dose–response relations in cultured spinal cord neurons (22), and we have used the lowest reported value, 2, to obtain a lower bound for r_{rec}. It should first be noted that if the necessary receptor population were restricted to the region delimited by the psd, with its radius of 0.1 μm, σ would have to be >60,000 μm^{-2}, which is appreciably above that which can be reasonably expected (13). Therefore, as shown in Fig. 1*B*, we have generated the relationship between N and r_{rec} for a range of binding site densities from 3750 to 30,000 μm^{-2}, the latter being the highest possible and probably an unreasonable value.‡

In every case, the radius of the receptor region required to incorporate at least 1000 channels is >0.1 μm. In particular, choosing σ = 15,000 as the maximal realistic value, the minimum r_{rec} = 0.206 μm, which is twice the radius of the psd, and the latter would, in turn, only accommodate 236 channels, a number 4 times less than our lowest estimate. Furthermore, these calculations incorporated the implicit assumption that all of the available channels are opened at the peak of the quantal response. Thus, this minimal radius is again too low, because such a saturation would be unprecedented. Indeed, the magnitude and time course of the quantal event depend not only on geometrical factors but

‡If σ = 30,000 μm^{-2}, the area per receptor–channel complex would be 67 nm^2. The maximal radius allowed in this space would be 4.1 nm, which is slightly less than that obtained by high resolution analysis of scanning transmission electron micrographs of tightly packed membrane-bound acetylcholine receptors from *Torpedo* (24). In addition, the maximal reported density of intramembranous particles, which have been observed with freeze fracture and assumed to correspond to single receptor–channel complexes, is only ≈10,000 μm^{-2}. At CNS junctions, particularly inhibitory ones, even lower values have been found (1).

also on the kinetics of transmitter diffusion and transmitter–receptor interactions (13, 14), which statistically requires that a fraction of the receptor–channel complexes available in the matrix will be unbound, single bound, or doubly liganded, and yet not activated.

The temporal properties of the quantal responses could only be assessed indirectly at these CNS junctions, because spontaneous individual events (*i*) may have arisen from multiple unidentified sources and (*ii*) rarely occurred (9). In contrast, the experimentally evoked unitary IPSPs represent the sum of quanta produced by several activated terminals; therefore, the question became whether the rise and decay times of these readily available larger potentials, or of their averages, adequately reflected the kinetics of the underlying quantal units. Fig. 2*A* indicates that the 80% peak times of IPSPs produced by neurons having 3–100 terminals on the M cell were very similar and ranged from 250 to 750 μsec (mean = 500 μsec; SD = 137 μsec; n = 59). The independence of rise time from this morphological variable would not be expected if release was asynchronous. The proposition that average responses accurately represented the quantal ones was further confirmed by comparing the kinetics of the large and small IPSPs produced by a single presynaptic neuron. In each experiment, a large number of unitary IPSPs was first collected and analyzed according to the binomial model (9) to evaluate the quantal size. Small and large responses were then separately selected and averaged for comparison with the mean. An example is shown in Fig. 2*B*; in this case, the average response had a mean quantal content of ≈5, while the average contents of the large and small ones were 7.8 and 2.8, respectively. Despite these differences, their 80% peak times and decay time constants were comparable. Likewise, another example in Fig. 2*C* shows that the 80% peak times were strikingly similar for mean quantal contents of 11.6, 6.6, and 4.3. These results strongly suggest that the parameters extracted from mean unitary responses do correspond to those of the underlying single components. Thus, quantal events could be modeled on the basis of information derived from the averaged IPSPs, which could be related to the time course of underlying conductance changes (10, 11) when the filtering effect of the M cell's time constant (200–400 μsec; ref. 25) was taken into consideration. Specifically, since the rise time of an IPSP is ≈500 μsec, that of the underlying conductance is in the range of 300 to 450 μsec; such a rise time has been observed with initial voltage clamp analyses of unitary inhibitory postsynaptic currents (unpublished observations), and was established as a necessary criterion of the model.

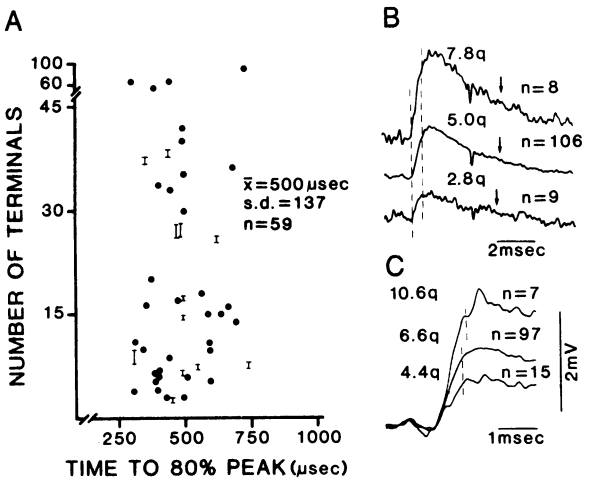

FIG. 2. Evidence that the time course of averaged unitary IPSPs in the M cell is representative of single quantal events. (*A*) Plot of the relationship between time to 80% peak amplitude of averaged unitary IPSPs evoked by impulses in single presynaptic interneurons and the number of active zones each cell established on the M cell, showing that the two parameters vary independently. Vertical bars signify the uncertainty in estimates of the number of terminals; morphological data are based on reconstructions in refs. 8 and 9. (*B* and *C*) Averaged responses from two experiments indicating that IPSP time courses were unchanged when large and small responses were analyzed separately. In *B*, the population average (n = 106) had a mean quantal content of 5.0 quanta (q), while that of the large and small responses was 7.8 and 2.8, respectively. The two dashed lines intersect the responses at their times of onset and 80% peak amplitudes. The decay time constants (arrows) were also relatively constant. In *C* (note expanded time scale), the dashed lines indicate that the 80% peak times for responses representing 6.6 and 4.4 q were the same, while this parameter was slightly longer for the larger responses (10.6 q). This constancy of waveform would not be expected if higher values of q reflected more temporal dispersion of transmitter release.

The computer simulation (Fig. 3*A*) reproduced the time course of the conductance change expected to underlie the experimentally recorded IPSPs (Fig. 3*B*). We first developed a model characterized by a restricted high density of receptors to determine a realistic lower bound on r_{rec}. Representative parameters satisfying the constraints described above were $k_{+1} = 4 \times 10^7$ (M-sec)$^{-1}$, $k_{-1} = 1600$ (sec)$^{-1}$, $k_{+2} = 4 \times 10^6$ (M-sec)$^{-1}$, and $k_{-2} = 160$ (sec)$^{-1}$, and the diffusion coefficient in the cleft was 2×10^{-6} cm^2/sec, which is smaller than that of free diffusion by a factor of 4. This model predicted that the full time course of the unitary response should be essentially independent of binding site density over the range of 3750 to 30,000 μm^{-2}, as illustrated for two representative values in Fig. 3*A*. This prediction was verified experimentally by recording IPSPs after iontophoresis of strychnine, which is an antagonist of glycine receptor-channel activation and could effectively reduce the binding site density. As shown in Fig. 3*B*, responses were indeed reduced in amplitude by 50%–80%, but their kinetics were unchanged (time to 80% peak = 500 ± 172 μsec in controls, and 540 ± 266 μsec after strychnine; n = 15). This result differs from

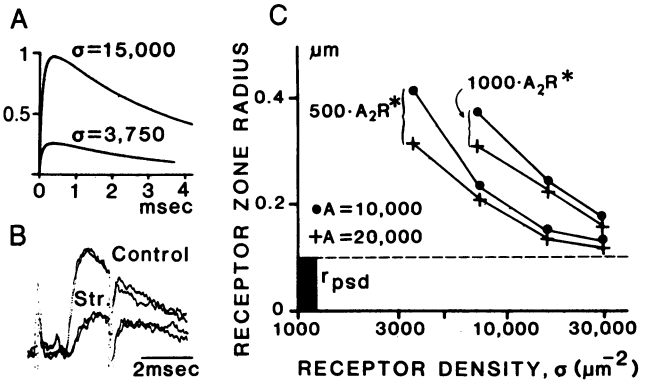

FIG. 3. Estimates of the receptor zone radius. (*A*) Time course of computer simulated responses for two binding site densities (σ, μm^{-2}) with r_{rec} = 0.23 μm, $r_{diffusion}$ = 0.46 μm, and the number of transmitter molecules per vesicle (A) = 10,000. The corresponding number of channels opened at the response peaks were 968 and 254, respectively. Solid lines plot the time course of the number of double-bound opened channels normalized with respect to the larger response. Note that the model predicts that response kinetics are independent of σ. (*B*) Unitary intracellular IPSPs recorded before (Control) and after iontophoresis of strychnine (Str.) had similar waveforms [two successive averages (n = 32) were superimposed for each case, to demonstrate stationarity]. (*C*) Estimates of receptor zone radius plotted as functions of σ, as derived from the kinetic (computer) model. Data are for two criterion responses—namely, 500 and 1000 double-bound opened channels (A_2R^*) at the IPSP peak, with (A) being either 10,000 or 20,000. The horizontal dashed line and the darkened bar represent the radius of the psd (r_{psd}).

that found at the neuromuscular junction, where the time course of the miniature endplate current depends on σ. The difference may reflect the fact that at the neuromuscular junction there is normally an excess of receptors, with the matrix extending far beyond the radius of the region containing binding sites equal in number to N—i.e., to the amount of transmitter molecules released, which defines the size of the so called "saturating disk" in the model of Land *et al.* (13, 14). In that configuration, blocking some receptors with an antagonist slows the rise of the endplate current because additional time is taken by the diffusion of some transmitter to reach distant available receptors. In contrast, with the present understanding of central synapses, the radius of the "saturating disk" (0.46 μm for σ = 15,000; N = 10,000) is appreciably larger than the derived r_{rec}. Hence, there are no marginal receptors beyond the area generating the responses in absence of the blockers.

The correspondence between the experimental and simulated data encouraged us to use the model to predict the characteristics of the synaptic disk consonant with the properties of intracellularly recorded IPSPs. Fig. 3*C* illustrates the derived relationship between σ and r_{rec} necessary for achieving a peak response of either 500 or 1000 open channels. It was not possible to match the physiological results unless r_{rec} was at least 20% larger than that calculated in Fig. 1*B*. Indeed, for a relatively high density of 15,000 μm^{-2}, r_{rec} was $\approx$0.23 μm for the criterion of 1000 open channels.

The model predictions in Fig. 3*C* provide a lower bound on r_{rec} of 0.23 μm, for conditions defined by slow diffusion and a high receptor density. A similar conclusion concerning the independence of rise time from binding site density was reached when the magnitude and time course of the unitary responses were simulated with a quite different set of parameters characterized by free diffusion and a low σ ($\leq$3750) but still with a surrounding receptor-free annulus. Then, the necessary radius of the receptor matrix became as high as 0.65 μm. Although this series of simulations used kinetic parameters quite different from the optimal values found for the case of a high receptor density, the two formulations led to common structural predictions, including that the total number of binding sites (1250 and 2500 in the first and second series, respectively) was much less than the number of transmitter molecules released as one quantum. These structural features would distinguish CNS synapses from the neuromuscular junction and again could account for the apparent constancy of response rise time after blocker application. In fact, we have obtained the same constancy of rise time when simulating fast endplate currents with the kinetics of acetylcholine binding, but with anatomical geometry and receptor disposition similar to those postulated here for the CNS synapses.

DISCUSSION

We conclude that the area encompassed by the receptor matrix at a CNS synapse is at least 4 times greater than that enclosed within the limits of the psd. Although our predictions are purposely conservative, particularly our estimate that 1000 channels are open at the peak of a quantal response (8, 9, 26), two possible sources of uncertainty nevertheless merit consideration. First, the idea that the psd cannot accommodate the number of channels opened at the peak of the quantal response would clearly be compromised if incorrect estimates of the single channel conductance, of the quantal conductance, or of the two together introduced an error factor of $\approx$4 (that is, if only $\approx$250 opened channels were required). For instance, that would be the case if single channel conductance equaled 180 pS. Even in this unlikely event, however, the kinetic modeling indicates that a maximum of $\approx$80% of the available channels could be doubly bound and activated at the peak of the response; thus, space for more channels would be still needed. Second, the estimated bounds on the size of the receptor matrix depend in part on the confirmation that the 80% rise time, t_c, of the quantal inhibitory postsynaptic current is independent of σ. This conclusion is valid to the extent that changes in t_c can be resolved with measurements of the voltage rise time, t_v, which is also influenced by the M cell's membrane time constant. We estimate that when t_c and the rise time of the membrane's voltage response to an instantaneous current pulse, t_m, are in the same range (300–400 μsec), a 30% increase in the current rise time should slow the voltage response by at least 20%, or 100 μsec [since empirically, $t_v = (t_m^2 + t_c^2)^{1/2}$]. Such an increase in IPSP rise time would most likely have been detected.

If the particle aggregates described with freeze fracture techniques can ever be correlated with receptors, their lower concentrations in peri-synaptic regions (2) would be indicative of a nonuniform (monotonically decreasing) distribution of receptors. In that case, the size estimates presented here would again be minimal. The present lack of a histochemical tool for directly visualizing receptors at these and other CNS synapses makes it difficult to draw final conclusions concerning the precise distribution of receptors. But the finding that the functional synaptic unit extends beyond the area limited by apparent structural specializations is consistent with the postulate that at these and other central synapses (8, 9, 27) the size of elementary responses attributed to one synaptic locus is quite invariant even though exocytosis presumably occurs randomly over the synaptic grid, which includes sites in apposition to the border of the psd.

At the neuromuscular junction, the postsynaptic membrane in apposition to a terminal (with numerous active zones) exhibits an essentially continuous psd and has a high density of receptors. (Then, extra-junctional receptors are truly outside the contact zone and cannot be expected to contribute to the endplate potentials.) At central synapses, the lack of correspondence between the functional receptor zone and the psd suggests that the localized nature of the latter no longer provides a sufficient rationale for assuming complete functional separation of discrete synaptic units. The alternative that, as at the neuromuscular junction, central synaptic units are not necessarily punctate might well provide a structural foundation for phenomena such as postsynaptic potentiation (4) and interaction between adjacent synapses (6).

We particularly thank Dr. B. R. Land for kindly providing the original computer model that made this work possible and for guiding us in implementing the necessary modifications. This work was supported in part by National Institutes of Health Grants NS15335 and NS17063, a Ralph Hochstetter Medical Research Advance Award to H.K. in honor of H. C. Buswell, and Institut National de la Santé et de la Recherche Médicale Grant C.R.L. 81.60.42.

1. Heuser, J. E. & Reese, T. S. (1977) in *Handbook of Physiology*, ed. Kandel, E. R. (Am. Physiol. Soc., Bethesda, MD), Vol. 1, Sect. 1, pp. 261–294.
2. Gulley, R. L. & Reese, T. S. (1981) *J. Cell Biol.* **91**, 298–302.
3. Gulley, R. L., Landis, D. M. D. & Reese, T. S. (1978) *J. Comp. Neurol.* **180**, 707–742.
4. Hartzell, H. C., Kuffler, S. W. & Yoshikami, D. (1975) *J. Physiol. (London)* **251**, 427–463.
5. Heidmann, T. & Changeux, J.-P. (1982) *C.R. Acad. Sci.* **295**, 665–670.
6. Korn, H. & Faber, D. S. (1983) *Soc. Neurosci. Abstr.* **9**, 465.
7. Korn, H. & Faber, D. S. (1976) *Science* **194**, 1166–1169.
8. Korn, H., Triller, A., Mallet, A. & Faber, D. S. (1981) *Science* **213**, 898–901.
9. Korn, H., Mallet, A., Triller, A. & Faber, D. S. (1982) *J. Neurophysiol.* **48**, 679–707.

10. Faber, D. S. & Korn, H. (1980) *Science* **208,** 612–615.
11. Faber, D. S. & Korn, H. (1982) *J. Neurophysiol.* **48,** 654–678.
12. Triller, A. & Korn, H. (1982) *J. Neurophysiol.* **48,** 708–756.
13. Land, B. R., Salpeter, E. E. & Salpeter, M. M. (1980) *Proc. Natl. Acad. Sci. USA* **77,** 3736–3740.
14. Land, B. R., Salpeter, E. E. & Salpeter, M. M. (1981) *Proc. Natl. Acad. Sci. USA* **78,** 7200–7204.
15. Fertuck, H. C. & Salpeter, M. M. (1976) *J. Cell Biol.* **69,** 144–158.
16. Peters, A., Palay, S. L. & Webster, H. deF. (1976) *The Fine Structure of the Nervous System* (Saunders, Philadelphia).
17. Young, A. B. & Snyder, S. H. (1973) *Proc. Natl. Acad. Sci. USA* **70,** 2832–2836.
18. Anderson, C. R. & Stevens, C. F. (1973) *J. Physiol. (London)* **235,** 655–691.
19. Kuffler, S. W. & Yoshikami, D. (1975) *J. Physiol. (London)* **251,** 465–482.
20. Diamond, J. & Roper, S. (1973) *J. Physiol. (London)* **232,** 113–128.
21. Werman, R. & Mazliah, Y. (1978) in *Iontophoresis and Transmitter Mechanisms in the Mammalian Central Nervous System*, eds. Ryall, R. W. & Kelly, J. S. (Elsevier/North-Holland, Amsterdam), pp. 400–402.
22. Sakmann, B., Hamill, O. P. & Bormann, J. (1983) *J. Neural Transm.* **18,** Suppl., 83–95.
23. Hamill, O. P., Bormann, J. & Sakmann, B. (1983) *Nature (London)* **305,** 805–808.
24. Zingsheim, H. P., Neugebauer, D.-Ch., Barrantes, F. J. & Frank, J. (1980) *Proc. Natl. Acad. Sci. USA* **77,** 952–956.
25. Fukami, Y., Furukawa, T. & Asada, Y. (1965) *J. Gen. Physiol.* **48,** 581–600.
26. Gold, M. & Martin, A. R. (1983) *Science* **221,** 85–87.
27. Jack, J. J. B., Redman, S. J. & Wong, K. (1981) *J. Physiol. (London)* **321,** 65–96.